Different signatures between chemically and biologically synthesized nanoparticles in a magnetic sensor: A new technology for multiparametric detection

E. Alphandery, L. Lijeour, Y. Lalatonne, L. Motte

▶ **To cite this version:**

E. Alphandery, L. Lijeour, Y. Lalatonne, L. Motte. Different signatures between chemically and biologically synthesized nanoparticles in a magnetic sensor: A new technology for multiparametric detection. Sensors and Actuators B: Chemical, 2010, 147 (2), pp.786-790. 10.1016/j.snb.2010.04.009 . hal-00704892

HAL Id: hal-00704892
https://hal.science/hal-00704892

Submitted on 26 Jun 2017

HAL is a multi-disciplinary open access archive for the deposit and dissemination of scientific research documents, whether they are published or not. The documents may come from teaching and research institutions in France or abroad, or from public or private research centers.

L'archive ouverte pluridisciplinaire **HAL**, est destinée au dépôt et à la diffusion de documents scientifiques de niveau recherche, publiés ou non, émanant des établissements d'enseignement et de recherche français ou étrangers, des laboratoires publics ou privés.

Different signatures between chemically and biologically synthesized nanoparticles in a magnetic sensor: A new technology for multiparametric detection

E. Alphandéry[×], L. Lijeour[+], Y. Lalatonne[⊥,‡], L. Motte[⊥]

×: Institut de minéralogie et de physique de la matière condensée (IMPMC), Université Pierre et Marie Curie, 140 rue de Lourmel, UMR 7590, CNRS, 75015, Paris, France.

+: Nanobacterie SARL, 36 boulevard Flandrin, F-75016, Paris, France.

⊥: Laboratoire CSPBAT. Université Paris 13, 74 Rue Marcel Cachin, F-93017, Bobigny, France.

‡ Service de Médecine Nucléaire, Hôpital Avicenne, APHP, Route de Stalingrad, F-93017, Bobigny, France.

Corresponding author: edouard.alphandery@impmc.jussieu.fr, edouardalphandery@hotmail.com

Keywords:

Magnetosome, magnetotactic bacteria, biosensor, Magnetic signature, multiparametric immunoassay, detectors, superparamagnetic nanoparticles, maghemite.

ABSTRACT: A magnetic sensor, called MIAplex, has been developed by the company Magnisense. This instrument measures a signal, which is proportional to the second derivative of a magnetization curve. We show that this sensor is able to discriminate between the signature of small superparamagnetic nanoparticles produced chemically and that of larger ferromagnetic nanoparticles produced by magnetotactic bacteria. The reason why this distinction is possible comes from the different magnetization curves of these two types of nanoparticles. These results pave the way for the simultaneous detection of different types of biological molecules or living organisms.

INTRODUCTION:

Although an enormous effort has been spent to develop new detection devices such as giant magneto-resistant (GMR) (1), spin valve (2), magnetoelastic sensors (3) or various types of magnetic sensors (4-9), a detector, which is able to detect simultaneously several different types of biological entities with a high sensitivity and a low cost is still lacking.

In this paper, we study a magnetic bio-sensor, called MIAplex^{r} (Magnetic Immuno Assays multiplex), which has been patented (10) and developed by the company Magnisense, (4-6). This sensor measures a signal, which is proportional to the second derivative of a magnetization curve. With this technique, a difference between the magnetization curves of different nanoparticles can easily be detected. Since the latter usually arises from a change in the nanoparticle sizes or interactions (5), one can imagine detecting simultaneously different types of biological entities by attaching them to nanoparticles, which are either prone to mutual interactions or possess different sizes. Such nanoparticles can either be chemically synthesized and functionalised (5) or produced biologically by magnetotactic bacteria (11, 12). Advantages of the biologically synthesized nanoparticles, called magnetosomes, reside in their large sizes, which result in a ferromagnetic behaviour at room temperature and strong dipolar interactions, the presence of a phospholipic membrane, which can be used to conjugate biological entities (12, 13) and their arrangement in chains of nanoparticles with aligned [111] crystallographic directions (14), which yield specific magnetic properties. The influence of the nanoparticle sizes and interactions on the MIAplex^{r} signal has previously been observed using maghemite superparamagnetic nanocrystals in powder forms (5). However, for the multiparametric detection of viruses, it is more suitable to use nanoparticles in solution than in powder. For this reason, nanoparticles produced by magnetotactic bacteria, called magnetosomes, which are larger, arranged in chains and therefore prone to dipolar

interactions in solution are studied in this paper. In order to examine the influence of the nanoparticle size on the MIAplex^{r} signal, the MIAplex^{r} signal of small nanoparticles is compared with that of larger magnetosomes. The influence of the nanoparticle interactions on the MIAplex^{r} signal is also assessed by studying several different types of samples containing either weakly interacting chains of magnetosomes, more strongly interacting single magnetosomes or a mixture of extracted single magnetosomes and chemically synthesized nanoparticles.

METHODS AND MATERIALS:

The instrument developed by the company Magnisense is called the MIAplex (multiplex Magnetic Immuno Assays). In this instrument, a magnetic material is exposed simultaneously to two alternative magnetic fields, a magnetic field of low frequency f_1 = 0.025 Hz and a magnetic field of higher frequency f_2 = 24.4 kHz. During the MIAplex measurements, the amplitude of the high frequency magnetic field (f_2) is fixed at a value lying between -8.88 Oe and 8.88 Oe, while the amplitude of the low frequency magnetic field (f_1) is varied between -452.4 Oe and 452.4 Oe. The second derivative of the magnetization curve of the material, d^2M/dH^2, is then recorded when the amplitude of the high frequency magnetic field is varied. Suppl. Figures 1(A) and 1(B) show two photographs of the MIAplex instrument. The two generators, generating the oscillating magnetic fields of frequencies f_1 and f_2 are shown in Suppl. Figure 1(A) together with the hollow cylinder in which the sample is positioned. The hollow cylinder is made of two coils, which generate the two different oscillating magnetic fields of frequencies f_1 and f_2 (Suppl. Figure 1(B)). As shown in the schematic diagram of Suppl. Figure 1(C), the ependorf tube containing the solution of nanoparticles is positioned at the center of the hollow cylinder.

The chemically synthezised nanoparticles are prepared following a protocol described previously (5). To prepare non-coated γFe_2O_3 particles, a solution of base (terbutylamine) is first added to an aqueous micellar solution of ferrous dodecyl sulfate ($Fe(DS)_2$) (0.61 g, 10^{-3} mol). The solution is then stirred vigorously for 2 hours at 28.5 °C and the resulting precipitate of uncoated nanocrystals is isolated from the supernatant by centrifugation. In the second step, the precipitate is washed with an acidic solution (HCl 10^{-1} mol.L^{-1}) and a solution of 5-hydroxy-5,5-bis(phosphono)pentanoic acid (HMBP-COOH) is used to coat the nanoparticles (n = 10^{-4} mol in 30 mL of water). The solution is stirred for two hours at room temperature. The precipitate that appears is washed with an acidic solution (HCl 10^{-1} mol.L^{-1}). Free HMBP-COOH are isolated from the coated particles using magnetic separation and centrifugation. The magnetic nanocrystals coated with HMBP-COOH molecules are finally dispersed in water. The pH, which is initially ~ 2, is progressively increased up to 7.4 by adding of solution of sodium hydroxide NaOH (10^{-1} mol.L^{-1}).

Magnetospirillum magneticum strain AMB-1, which belongs to α-Proteobacteria (12) was purchased from the ATCC (ATCC 700274). Cells were grown microanaerobically at room temperature (~25°C) in liquid culture in MSGM medium (ATCC Medium 1653). Iron ions (Fe^{2+} or Fe^{3+}) were introduced in the growth medium using an iron quinate solution. They were incorporated by the bacteria within an intracellular vesicle yielding the formation of the magnetosomes through a mechanism, which has previously been described but is still not fully understood (16). Details about the growth of these bacteria including their growth curve can be found elsewhere (17). Cells were harvested at stationary phase. Stationary phase occurred when the medium became completely reduced as indicated by a change in the coloration of the growth medium, from pink to colorless. Note that in order to maximize the number of magnetosomes synthesized per bacteria and to minimize the magnetosome size distribution, strictly anerobic conditions can be used instead of microanerobic growth

conditions. Two different types of samples were prepared. The living bacteria were first centrifuged at 8000 rpm for 15 minutes. The solution was then placed against a magnet and the supernatant containing the growth medium was removed and replaced by 2 ml of deionized water. Hence we obtained 2 ml of a solution of whole bacteria dispersed in water, which we redispersed in a 10 mM Tris buffer and sonicated during 60 minutes at 30 W to extract the chains of magnetosomes from the whole bacteria. After sonication the solution containing the extracted chains of magnetosomes was placed against a magnet and the supernatant was removed to get rid of most of the biogenic material. The solution was washed 10 times in this way. 1 ml of this solution was transferred into an ependorf tube and was not treated further. It contained the extracted chains of magnetosomes (14). 1 ml of the same solution was transferred in another ependorf tube and heated for one hour at 90 ^{0}C in the presence of 1 % sodium dodecyl sulfate (SDS). The solution was heated by placing the ependorph inside boiling water. The second solution contained the individual magnetosomes, which were both extracted from the whole bacteria and detached from the chains (14).

The nanoparticles chemically synthesized, the individual magnetosomes and the extracted chains of magnetosomes are characterized using transmission electron microscopy (TEM), infrared measurements (Nicolet 380 FT IR Thermo Electro Corporation), U. V. spectroscopy (Cary 50 Scan Varian). TEM is used to determine the sizes of the nanoparticles. FTIR spectroscopy is used to confirm nanocrystal surface complexation via phosphonate groups for the chemically synthesized nanoparticles. A method described in the supplementary section and in ref. 18 is used to determine that the composition of the magnetosomes is maghemite. The concentration of the nanoparticles is estimated using U. V. spectroscopy. Finally, to measure the weight and hence the concentration of the different solutions of nanoparticles, the latter are first freeze dried to eliminate water and then weighted.

RESULTS AND DISCUSSION:

Typical magnetization curves as well as their first and second derivatives are shown in Suppl. Figures 2(A) to 2(C) for small superparamagnetic nanoparticles and in Suppl. Figures 2(D) to 2(F) for large ferromagnetic nanoparticles. For these two types of nanoparticles, a different magnetization curve is expected as shown in Suppl. Figures 2(A) and 2(D). This yields a difference both in the first derivative (Suppl. Figures 2(B) and 2(E)) and second derivative (Suppl. Figures 2(C) and 2(F)) of the magnetization curves. The second derivative of the magnetization curve goes through 0 for the superparamegnetic nanoparticles (Suppl. Figure 2(C)), while this is not the case for ferromagnetic nanoparticles (Suppl. Figure 2(F)), making it a criterion of differentiation between the two signatures.

Figures 1(A) and 1(B) show the TEM image and the MIAplex^{r} signature of the small chemically synthesized superparamagnetic nanoparticles. The average size of these nanoparticles is estimated as ~ 13.4 nm. Comparing the FTIR spectra of γFe_2O_3 nanocrystals coated with HMBP-COOH (Suppl. Figure 3, red curve) with those of the nanoparticles coated with free HMBP COOH molecules (Suppl. Figure 3, blue curve), large changes are observed within the P-O stretching region (1200-900 cm^{-1}) whereas the carboxylate region (1600-1400 cm^{-1}) remains unchanged. These results are in agreement with previous work and indicate that HMBPs are grafted onto the nanocrystal surface through the phosphonate groups (15, 19). Consequently the large number of COOH functionalities at the outer surface of the magnetic core of the nanoparticles act as precursor groups for the covalent coupling of biomolecules such as antibodies. The BP functions complex the nanocrystal surfaces and carboxylate groups at the outer surface of the nanoparticles induce electrostatic repulsions between the nanoparticles, weakening their mutual interactions. As show in Figure 1(B), the MIAplex^{r} signal is similar to that expected for assemblies of non interacting superparamagnetic nanoparticles (Suppl. Figure 2(C)). It goes through 0 whereas for assemblies of interacting

superparramagnetic nanoparticles, the MIAplex signal should widens and not go through 0 (5).

In order to enhance the interactions between the nanoparticles, we study magnetosomes produced by magnetotactic bacteria, which are significantly larger (~ 50 nm in mean diameter) than the chemically synthesized nanoparticles. We study two types of magnetosome arrangements, the chains of magnetosomes and the individual magnetosomes, which are both extracted from the whole bacteria. TEM images of each of these two types of sample are shown in Figures 2(A) and 2(B). As shown in these two Figures, the chains of magnetosomes form weakly interacting assemblies (Figure 2(A)) whereas the individual magnetosomes form more compact assemblies of aggregated and more strongly interacting magnetosomes (Figure 2(B)). Fifty microliters of a solution containing either the chains of magnetosomes or the individual magnetosomes and 2 10^{-3} % by weight of maghemite (14, 18) are deposited on top of a silica substrate for magnetic measurements. The magnetization curves of the two samples are shown in Figure 2(C). As shown in this Figure, the magnetization curve of the chains of magnetosomes (red curve) saturates more rapidly than that of the single magnetsosomes (black curve). Despite this feature, the magnetization curves of these two samples are too similar to produce a pronounced difference between their calculated second derivatives. Indeed, as shown in Figure 2(D), the second derivative of the magnetization curve of the chains of magnetosomes (red curve) is very similar to that of the single magnetosomes (black curves). We examine if the MIAplex^{r} instrument enables a more sensitive detection of the nanoparticle interactions. For that, we compare the MIAplex^{r} signal of 50 μl of a solution containing chains of magnetosomes with that of 50 μl of a solution containing individual magnetosomes. By contrast to what is observed in Figure 2(D), the MIAplex^{r} signatures of these two solutions shown in Figure 2(E) are different. For the single magnetosomes, which are more strongly interacting than the chains of magnetosomes, the MIAplex^{r} signal (Figure

2(E), black line) is wider than that of the chains of magnetosomes (Figure 2(E), red line). From these results, we can conclude that the MIAplex^{r} instrument provides a more sensitive technique to detect the interactions between nanoparticles than the measurement of a magnetization curve or of the estimate of its second derivative.

In order to confirm the influence of the nanoparticle interactions on the MIAplex^{r} signal, we study a mixture of individual magnetosomes and chemically synthesized nanoparticles in various proportions. The first solution contains 50 % of individual magnetosomes and 50 % of chemically synthesized nanoparticles. In this case, Figure 3(A) shows that the MIAplex^{r} signal of the mixed solution (black curve) is similar to the average MIAplex^{r} signal, which is the sum of the MIAplex signals of the chemically synthesized nanoparticles and individual magnetosomes divided by 2 (red curve). The amount of magnetosomes is not sufficiently large to modify the interactions in the mixed solution. Therefore, we use a solution, which contains a higher percentage of magnetosomes (80 %) and a lower percentage of chemically synthesized nanoparticles (20 %) in order to favor the presence of interactions in the solutions containing the magnetosomes. The MIAplex^{r} signal of the mixture of the two solutions is shown in Figure 3(B) (black line). It is different from the MIAplex^{r} signal, which is the sum of the signals of the chemically synthesized nanoparticles and extracted magnetosomes divided by two (red line). We hypothesize that in the presence of the small nanoparticles, the magnetosomes are less interacting with each other. This could be due to the insertion of the small nanoparticles between the magnetosomes. The decrease of the interactions between the magnetosomes in the mixed solution would cause the MIAplex^{r} signal to narrow as observed by comparing the two plots (dark line and red line).

CONCLUSION:

In this paper, we have shown that the large magnetosomes biosynthesized by magnetotactic bacteria produce a different MIAplex^{r} signal than the small nanoparticles synthesized chemically. This paves the way for the use of the MIAplex^{r} instrument for multiparametric detection. In addition, we have shown the influence of the nanoparticle interactions on the MIAplex signal. We have established that an increase in the interactions between the magnetosomes results in the widening of the MIAplex^{r} signal. Hence, we can hypothesize that the presence of biological molecules, such as antibodies or viruses, bound at the surface of the magnetosomes, will also modify the magnetosome interactions and hence their MIAplex^{r} signatures. These experiments are in progress and should allow for the detection of two or several different biological molecules. A detection skeem, which would enable the detection of two biological entities, is described in the supplementary information section.

Acknowledgement:

This work was funded by the French company Nanobacterie, SARL, through a partnership involving another French company, Magnisense, the University Pierre et Marie Curie and the University Paris XIII. We thank Rodolphe Dubois for his help with the TEM measurements.

Figures:

Figure 1: (A): TEM micrographs of the chemically synthesised nanoparticles deposited on top of a TEM grid. (B): MIAplex^{r} signal of the chemically synthesised nanoparticles

Figure 2: TEM micrographs of the extracted chains of magnetosomes (A) and single magnetosomes (B) deposited on top of a TEM grid. (C): Magnetization curve of the extracted chains of magnetosomes and extracted individual magnetosomes. (D): The second derivative of the magnetization curve. (E): The MIAplex^{r} signal of the extracted chains of magnetosomes and extracted individual magnetosomes. In (C), (D) and (E), the red and black lines represent the signals of the extracted chains of magnetosomes and individual magnetosomes respectively.

Figure 3: (A): The MIAplex^{r} signal of a solution containing 50 % of individual magnetosomes and 50 % of chemically synthesized nanoparticles (black line). The average signal, which is the sum of the MIAplex^{r} signals of the extracted individual magnetosomes and chemically synthesized nanoparticles divided by 2 (red line). (B): Same as in (A) for a solution containing 80 % of individual magnetosomes and 20 % of chemically synthesized nanoparticles.

Supplementary Figure 1: (A): A photograph of the MIAplex^{r} instrument showing the two power supplies generating the two alternative currents as well as the hollow cylinder in which the sample is positioned for magnetic measurements. (B): A photograph of the hollow cylinder showing that the latter possesses two coils generating the oscillating magnetic fields of frequency f_1 and f_2. (C): A schematic diagram showing the ependorf tube, which contains the solution to be measured and is positioned at the centre of the hollow cylinder.

Supplementary Figure 2: The magnetization curve, (A), first derivative of the magnetization curve, (B), and second derivative of the magnetization curve, (C) for small superparamagnetic nanoparticles chemically synthesized. (D), (E), (F): Same as in (A), (B), (C) for larger ferromagnetic magnetosomes. The magnetization curves in (A) and (D) are typical to those expected for superparamagnetic and ferromagnetic nanoparticles respectively while the first and second derivatives shown in the other Figures are calculated.

Supplementary Figure 3: Infrared spectra of the chemically synthesised nanoparticles (red curve) and free HMBP-COOH molecules (blue curve).

References

[1] Janssen, X. J. A.; Van Ijzendoorn, L. J.; Prins, M. W. J.; 2008. Biosens. Bioelectron. 23, 833-838.

[2] Graham, D. L.; Ferreira, H. A.; Freitas, P. P.; Cabral, J. M. S.; 2003. Biosens. Bioelectron. 18, 433-488.

[3] Huang, S.; Yang, H.; Lakahmanan, R., S. ; Johnson, M. L.; Wan, J.; Chen, I.-H.; Wikle, H., C.; Petrenko, V. A.; Barbaree, J., M.; Chin, B., A.; 2009 Biosens. Bioelectron. 24, 1730-1736.

[4] Lenglet, L.; 2009. J. Magn. Magn. Mater. 321, 1639-1643.

[5] Lalatonne, Y.; Benyettou, F.; Bonnin, D.; Lièvre, N.; Monod, P.; Lecouvey, M.; Weinmann, P.; Motte, L. 2009. J. Magn. Magn. Mater. 321, 1653-1657.

[6] Nitikin, P. I.; Vetoshko, P. M.; Ksenevich, T. I.; 2007. J. Magn. Magn. Mater. 311, 445-449.

[7] Miller, M. M.; Sheehan, P. E.; Edelstein, R. L.; Tamanaha, C. R.; Zhong, L. S.; Bounnak, L.; Whitman, L. J.; Cotton, R. J.; 2001. J. Magn. Magn. Mater. 225, 156-160.

[8] Chemla, Y. R.; Grossman, H. L.; Poon, Y.; McDermott, R.; Stevens, R.; Alper R.; and Clarke, J.; 2000. Proc. Natl. Acad. Sci. 97, 14268-14272.

[9] Ferreira, H. A.; Graham, D. L.; Freitas, P. P.; and Cabral, J. M. S.; 2003. J. Appl. Phys. 93, 7281-7286.

[10] P.I. Nikitin, P.M. Vetoshko, Patent of Russian Federation RU 2166751 (09.03.2000), EP 1262766 publication, 2002.

[11] For a comprehensive review on magnetotactic bacteria, see: Bazylinski, D. A.; Frankel, R. B.; 2004. Nat. Rev. Microbiol. 2, 217-230.

[12] Arakaki, A.; Nakazawa, H.; Nemoto, M.; Mori, T.; Matsunaga, T.; 2008 J. R. Soc. Interface 5, 977-999.

[13] Kuhara, M.; Takeyama, H.; Tanaka, T.; Matsunaga, T.; 2004. Anal. Chem. 76, 6207-6213.

[14] Alphandéry, E.; Ding, Y.; Ngo, A. T.; Wu, L. F.; Pileni, M. P.; 2009 ACS Nano 3, 1539-1547.

[15] Lalatonne, Y.; Paris, C.; Serfaty, J. M.; Weinmann, P.; Lecouvey, M.; and Motte, L.; 2008 Chem. Commun. 22, 2553-2555

[16] Faivre, D.; Schüler, D.; 2008. Chem. Rev. 108, 4875-4898.

[17] Yang, C., D.; Takeyama, H.; Tanaka, T.; Matsunaga, T.; 2001 Enz. Microb. Techno. 29, 13-19.

[18] Alphandéry, E.; Ngo, A. T.; Lefèvre, C.; Wu, L. F.; Pileni, M. P.; 2008 J. Phys. Chem. B 112, 12304-12309.

[19] Benyettou, F.; Lalatonne, Y.; Sainte-Catherine, O.; Monteil, M.; Motte, L. International Journal of Pharmaceutics, (DOI: 10.1016/j.ijpharm.2009.04.010)

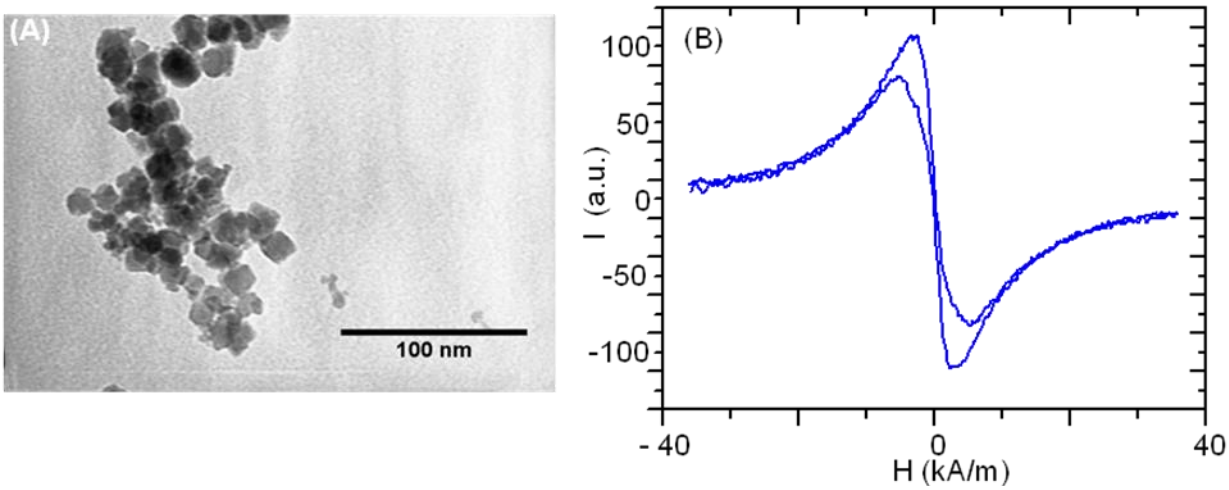

Figure 1.

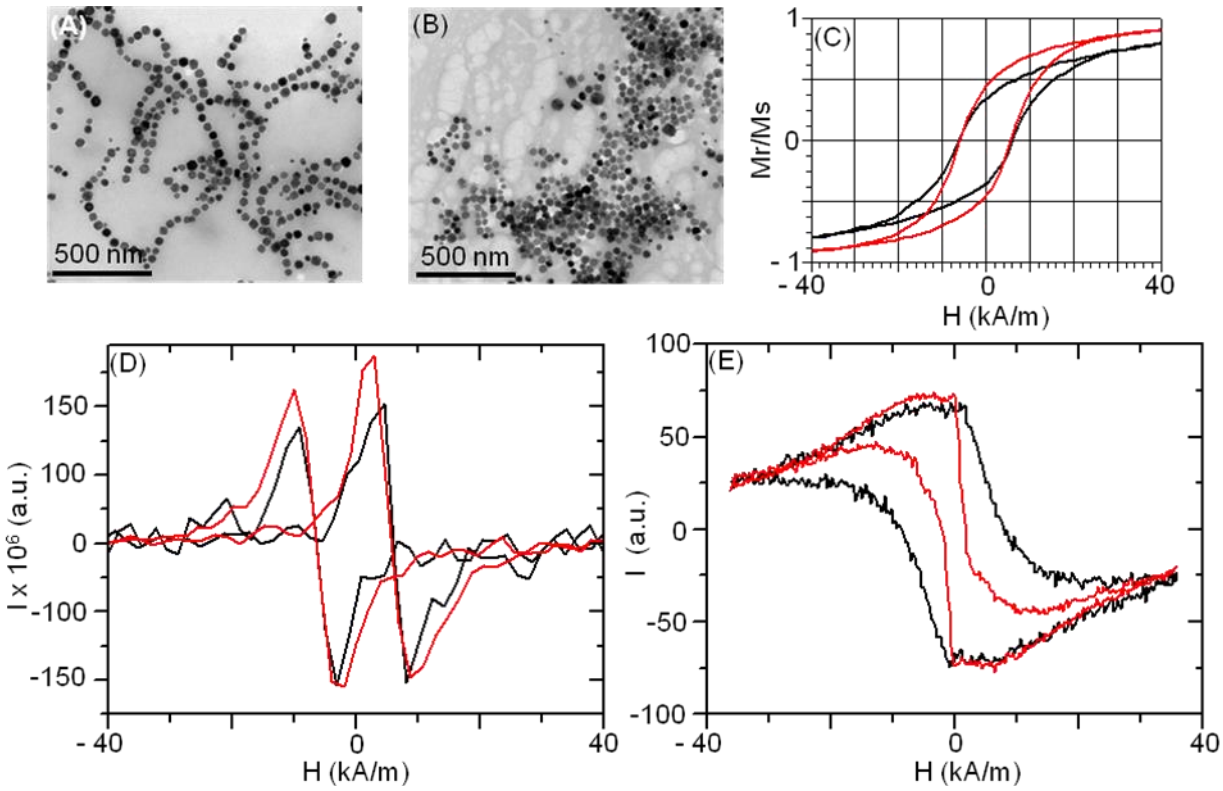
(A)
500 nm
(B)
500 nm
(C)
Mr/Ms
1
0
- 1
- 40
0
40
H (kA/m)
(D)
I x 10⁶ (a.u.)
150
100
0
-100
-150
- 40
0
40
H (kA/m)
(E)
I (a.u.)
100
50
0
-50
-100
- 40
0
40
H (kA/m)

Figure 2.

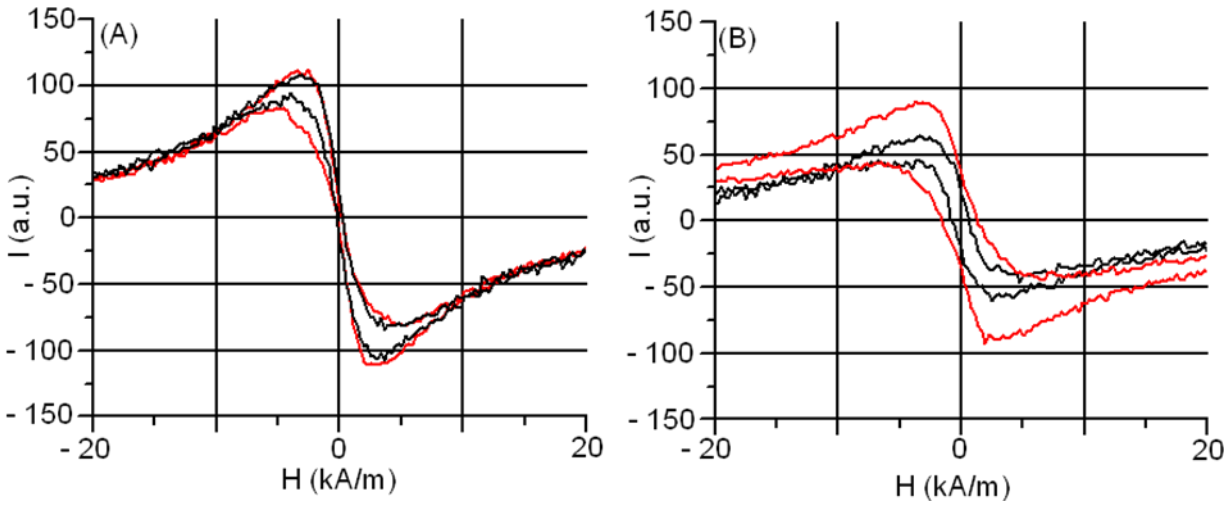
(A)
150
100
50
0
- 50
- 100
- 150
I (a.u.)
- 20
0
20
H (kA/m)
(B)
150
100
50
0
- 50
- 100
- 150
I (a.u.)
- 20
0
20
H (kA/m)

Figure 3.

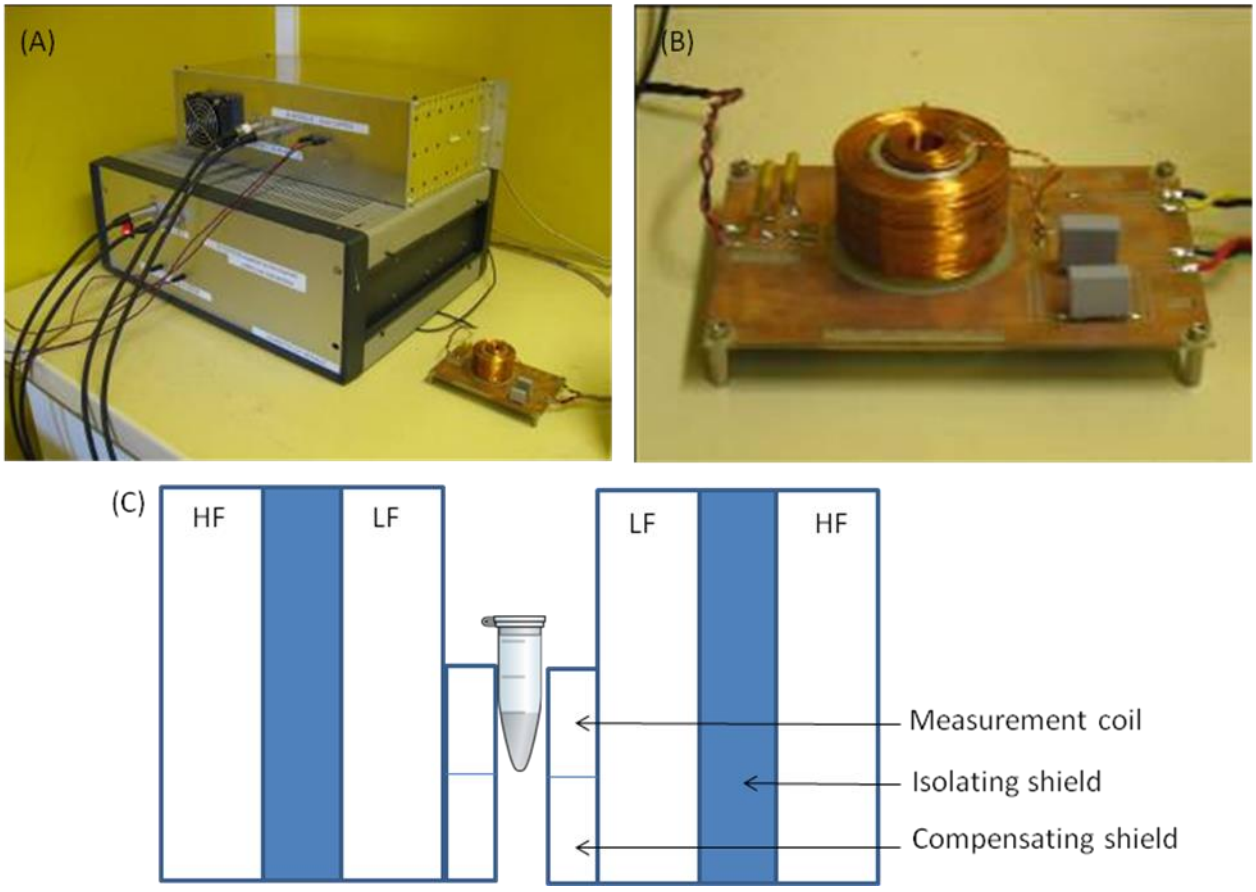
(A)
(B)
(C)
HF
LF
LF
HF
Measurement coil
Isolating shield
Compensating shield

Suppl. Fig. 1

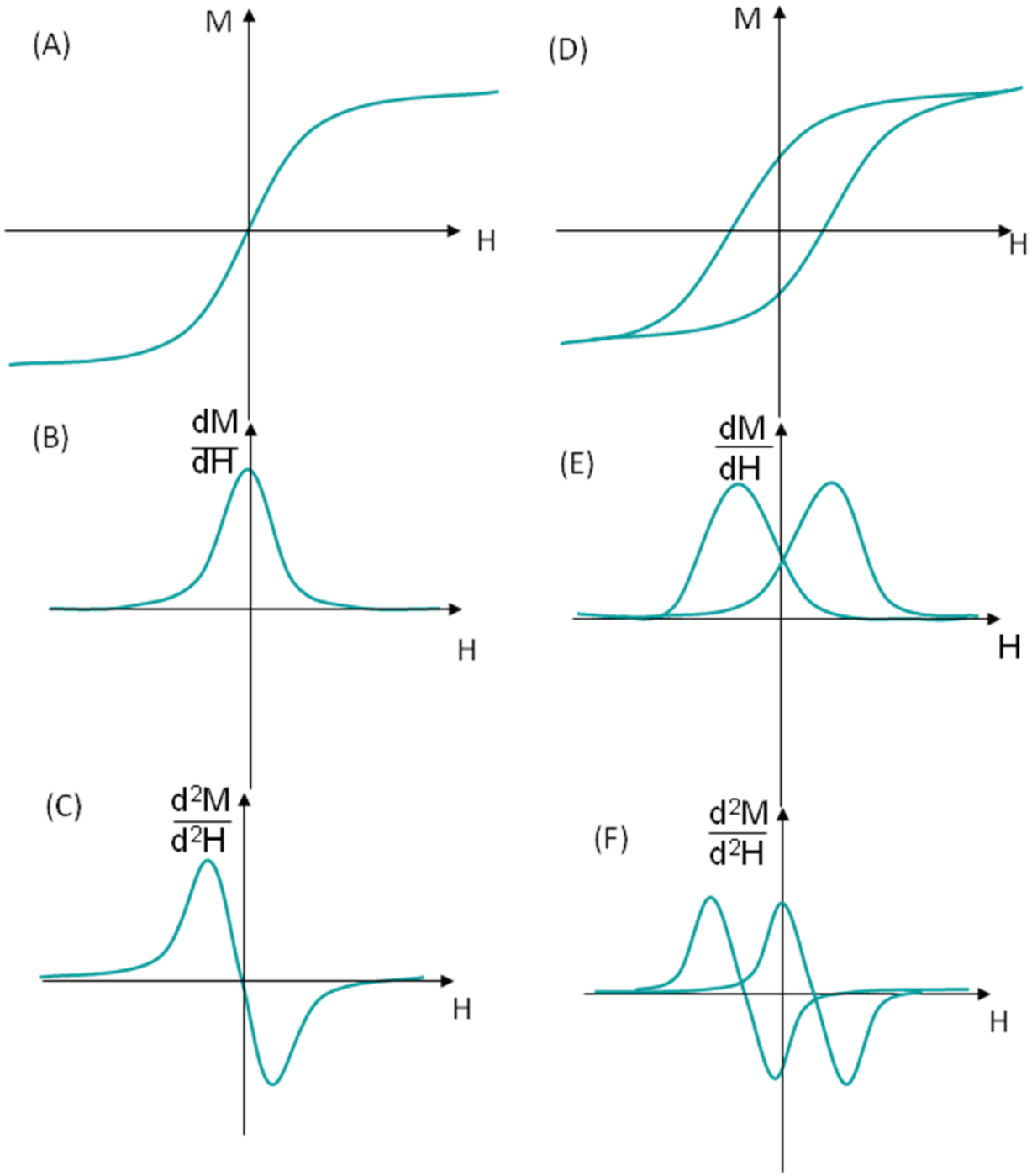

Suppl. Fig. 2

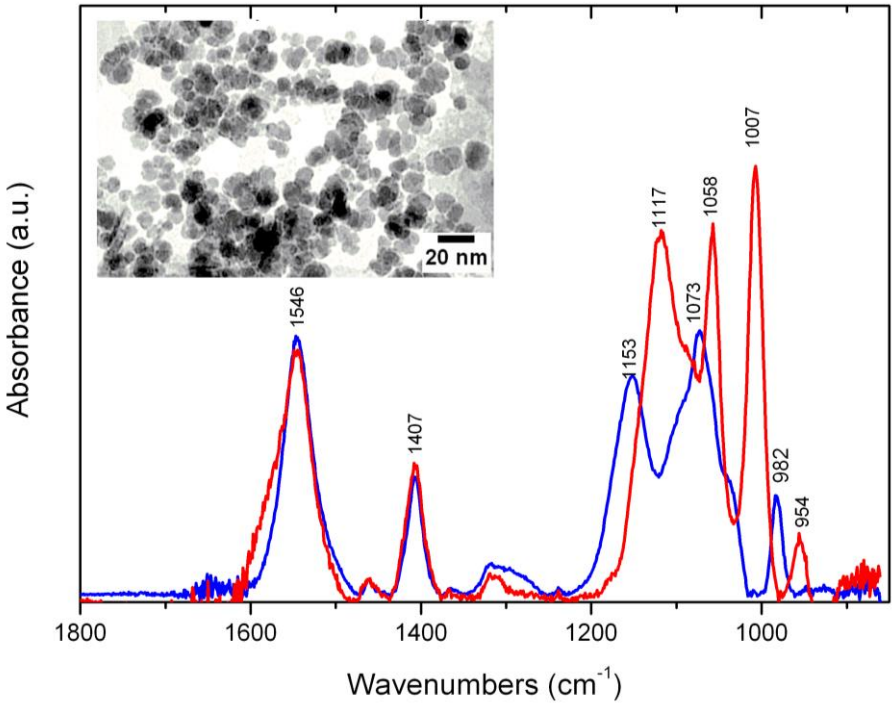
Absorbance (a.u.)
20 nm
1546
1407
1153
1117
1073
1058
1007
982
954
1800
1600
1400
1200
1000
Wavenumbers (cm-1)

Suppl. Fig. 3

Supplementary information: Composition of the magnetosomes.

The magnetosomes are either made of magnetite or maghemite. We know that from the electron diffraction pattern measured on an assembly of magnetosomes. From Figure (C) below (Alphandery et al, J. Phys. Chem. C 2008, Vol. 112, P. 12304-12309), we deduced that the magnetosomes were composed of either maghemite or magnetite and not of other iron oxides.

From this electron diffraction pattern (Figure (C)), it is not possible to distinguish between magnetite and maghemite. To make this distinction, we measured the saturating isothermal remanent magnetization (SIRM) curve of the magnetosomes. This technique enables a distinction between maghemite and magnetite to be made. The Verwey transition is only present in magnetite and not in maghemite. Since we didn't observe the Verwey transition in the SIRM signal of the extracted magnetosomes (Figure (D)), we knew that the magnetosomes were made of maghemite and not magnetite.

The composition of the magnetosomes essentially depends on their level of exposition to oxygen. Since we leaved the whole bacteria or the magnetosomes extracted from the bacteria exposed to air for a long time, the magnetosomes oxidized in maghemite. Since maghemite and magnetite have very similar magnetic properties at ambient temperature, the oxidation of the magnetosomes in maghemite is not really a problem for the type of application that we want to develop.

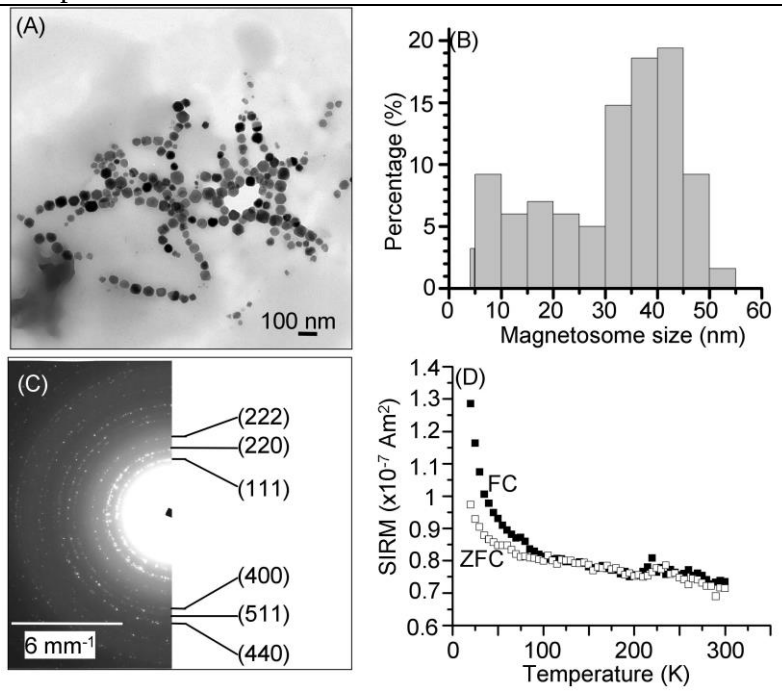

Fig. 5

Figure: (A) TEM image obtained for the extracted magnetosomes deposited on top of a TEM grid. (B) Histogram showing the size distribution of the magnetosomes. (C) TEM electron diffractogram of the extracted magnetosomes. (D) SIRM of the FC (O) ZFC (□) of the sample containing the extracted magnetosomes (Alphandery et al, J. Phys. Chem. C 2008, Vol. 112, P. 12304-12309).

Supplementary information: Detection skeem for the detection of two biological entities.

The attachment of biological entities to the nanoparticles is not a major difficulty. It can be realized with the magnetosomes because of the presence of the phospholipic membrane and with the chemically synthesized nanoparticles because of the BPCOOH molecules grafted at the surface. There are two ways in which a multiparametric detection of two biological entities can be realized:

(i) The two biological entities (BE1) and (BE2) that we want to detect can be bound to the chemically synthesized nanoparticles (CSN) and magnetosomes (M). The solution containing CSN/BE1 and M/BE2 is then poured within our Miaflow using a technology developed by the company Magnisense. CSN/BE1 and M/BE2 get then bound to a solid support. The presence of BE1 and BE2 is detected using the Miaplex. The Miaplex signals of CSN/BE1 and M/BE2 should be different since the Miaplex signal of CSN and M are different. This would enable the multiparametric detection of BE1 and BE2.

(ii) The two biological entities (BE1) and (BE2) we want to detect are bound to the chemically synthesized nanoparticles (CSN) and magnetosomes (M). The Miaplex signal of the solution containing CSN/BE1 and M/BE2 is measured. Due to the strong interactions between the magnetosomes, we expect that the signal of the solution containing CSN/BE1 and M/BE2 will be different from that containing only CSN and M, hence providing a means for the multiparametric detection of BE1 and BE2.

We are planning to carry out experiments to verify (i) and (ii) next. We have added in the supplementary information section the two ways in which the multiparametric detection of BE1 and BE2 could be realized.